

# Observations of reversible and irreversible structural transitions of cobalt on Si (1 1 1) with LEEM

**Phaneuf, R.J.; Hong, Y.; Horch, Sebastian; Bennett, P.A.**

*Published in:*
Micron

*Link to article, DOI:*
10.1016/S0968-4328(98)00040-7

*Publication date:*
1999

PERGAMON

Micron 30 (1999) 13–20

micron

# Observations of reversible and irreversible structural transitions of cobalt on Si (1 1 1) with LEEM

R.J. Phaneuf[a,*], Y. Hong[b], S. Horch[b], P.A. Bennett[b]

[a]*Department of Physics and Astronomy, University of Maryland and Laboratory for Physical Sciences, College Park, MD 20742-4111, USA*
[b]*Department of Physics and Astronomy, Arizona State University, Tempe, AZ 85287-1504, USA*

Received 2 February 1998; received in revised form 27 May 1998; accepted 2 June 1998

**Abstract**

We present real time images of the evolution of the structure of the Si (1 1 1) surface during the deposition of cobalt at elevated temperatures, acquired using low-energy electron microscopy. The system follows a sequence of coexisting ordered and disordered phases, consistent with two-dimensional eutectic behavior. Reversible temperature driven transitions are observed between the ordered Si (1 1 1)–$(7 \times 7)$ reconstructed phase and a disordered lattice gas of Co-containing ring-clusters (RC), indicating a local equilibrium between these structures. Only irreversible temperature driven transitions from an ordered $(\sqrt{7} \times \sqrt{7})$-RC phase to the disordered phase are observed. The nucleation and growth of stable islands, mostly $CoSi_2$, depletes the Co-rich $(\sqrt{7} \times \sqrt{7})$ structure of Co, resulting in the formation and growth of adjacent regions of the Co-poor disordered ''$(1 \times 1)$''-RC phase. 

*Keywords:* Surfaces; Surface phase transitions; Surface phase separation; Silicides; Electron microscopy; Low-energy electron microscopy

## 1. Introduction

The development of a number of new surface sensitive electron microscopies over the past 10–15 y has revolutionized how phenomena at surfaces are studied. Rather than determining structures by relying on the comparisons between the results of scattering experiments and calculations based on an assumed, often incomplete model, these techniques make it possible to image both the structural and compositional variations on a surface directly. The best known of these microscopies, scanning tunneling microscopy (STM) allows the measurement of structure at surfaces down to the single atom-scale. Low-energy electron microscopy (LEEM) offers a more modest spatial resolution than STM, typically several nanometers, but as it is a true imaging technique, it allows for better temporal resolution. In addition, the spatial separation of the sample from the objective lens, millimeters compared to nanometers between the sample and tip in STM, makes it relatively easy to acquire in situ images over a wide range of temperature, and during exposure of the sample to evaporative fluxes during growth, and various gas or ion sources.

LEEM has frequently been used to study the evolution of structure on silicon surfaces (Bauer et al., 1991; Mundschau et al., 1989; Swiech and Bauer, 1991; Bartelt and Tromp, 1996; Bartelt et al., 1996; Theis and Tromp, 1996; Phaneuf et al., 1991; 1992; 1993), in part because of the dominating role of silicon in the microelectronics technology. Among those processing steps which are most basic and important in silicon device fabrication, is the formation of metal–silicon interfaces, which are used for making electrical contacts. The transition metals are of particular interest, as they allow the formation of stable silicide compounds (Tu and Mayer, 1978; Nicolet and Lau, 1983; Reader et al., 1993). Recently, the importance of surface and interface structures in silicide-forming structures was demonstrated (Bennett et al., 1992b; 1994). For example, the growth of thin film overlayers can be significantly altered using monolayer template and/or low-temperatures, to produce useful metastable structures (Tung, 1992; Tung and Batstone, 1988). Bennett et al. used both the room temperature STM and ion scattering to characterize stable ring-cluster (RC) structures which exist for transition metals on Si (1 1 1) (Bennett et al., 1992a). Their studies did not allow the direct observation of the formation of RC phases at the elevated temperatures used during deposition however, a task for which the real time, in situ imaging capabilities of the LEEM are ideally suited.

In this article, we present the results of a real-time

* Corresponding author.

0968–4328/99/$ - see front matter 
PII: S0968-4328(98)00040-7

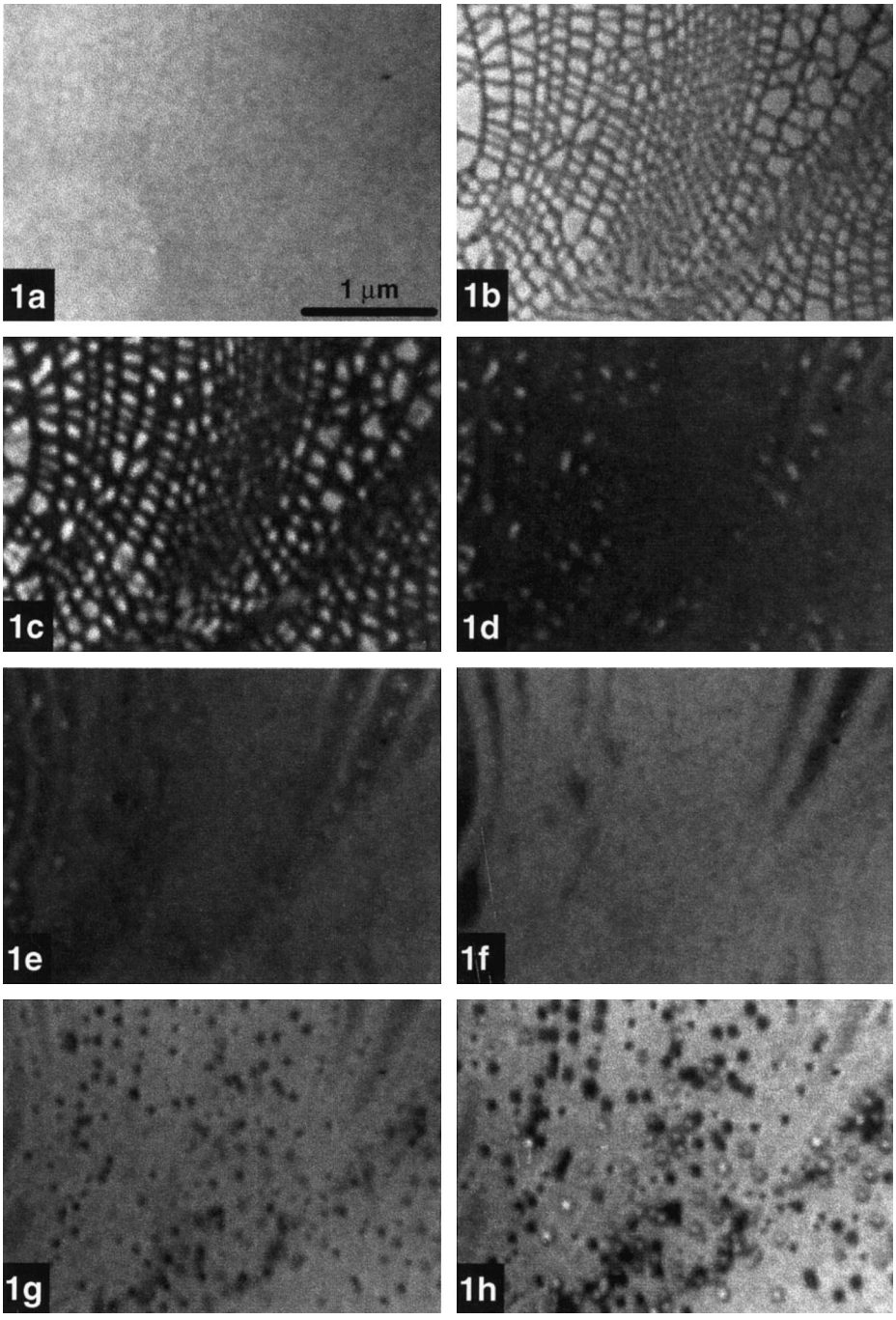


Fig. 1. LEEM images of Si (1 1 1) acquired during the deposition of Co showing a progression of structural phases. Temperature $T = 735$°C. Incident flux $F_{Co} = 0.0018$ ML/s. Incident energy $E_i = 3.6$ eV. Normal incidence. Scale bar shows 1 μm. (a) $\Theta_{Co} = 0.00$ ML, the uniform $(7 \times 7)$ reconstructed phase appears as light gray at these imaging conditions, (b) $\Theta_{Co} = 0.02$ ML. The disordered ''$(1 \times 1)$''-RC appears as black at these conditions, along step edges and $(7 \times 7)$ domain boundaries, (c) $\Theta_{Co} = 0.04$ ML, (d) $\Theta_{Co} = 0.10$ ML, (e) $\Theta_{Co} = 0.11$ ML. The ordered $(\sqrt{7} \times \sqrt{7})$-RC phase appears as dark gray at these conditions, (f) $\Theta_{Co} = 0.14$ ML, (g) $\Theta_{Co} = 0.18$ ML, ''$(1 \times 1)$''-RC depletion zones appear as black circles, (h) $\Theta_{Co} = 0.22$ ML,$CoSi_2$ islands visible as white regions within black ''$(1 \times 1)$''-RC depletion zones.

LEEM study of the surface phases which are formed during the first stages of the deposition of cobalt on the (1 1 1) surface of silicon. Parts of these results have been reported elsewhere (Phaneuf et al., 1997). We observe both reversible and irreversible structural changes, driven by varying either the surface cobalt-coverage or the temperature. Finally, we discuss a model of this system based on a local equilibrium between surface phases in competition with the formation of the stable bulk silicide phase.

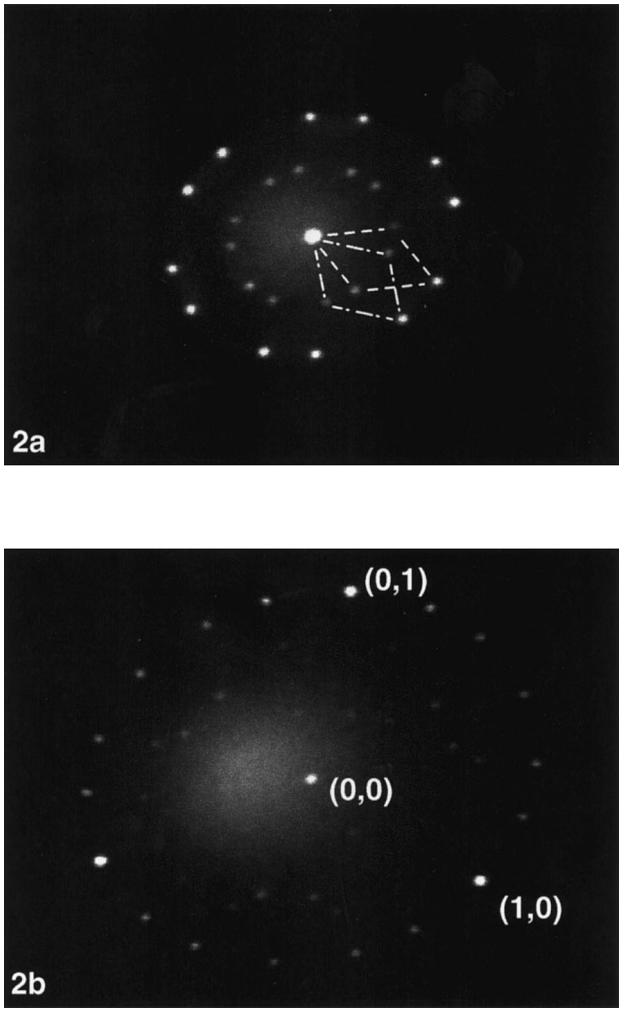


Fig. 2. ($\sqrt{7} \times \sqrt{7}$)-LEED pattern observed for the region of the Co/Si (1 1 1) surface shown in Fig. 1. $\Theta_{Co} = 0.22$ ML. Temperature quenched down to near room temperature. (a) $E_i = 6.7$ eV. Reciprocal unit meshes for ($\sqrt{7} \times \sqrt{7}$) R $\pm$ 19.1° are shown by dashed and dot-dashed lines, (b) $E_i =$ 15.7 eV. Integer-order beams, corresponding to bulk Si (1 1 1) periodicity, are labeled. Normal incidence for both panels. The elliptical appearance of the pattern is an electron-optical artifact produced by the mode in which the ''magnetic prism'' was operated. The diffuse intensity results from inelastically scattered electrons.

## 2. Materials and methods

The technique used here, LEEM, was developed by Bauer, and has been the subject of recent reviews (Bauer, 1994; Veneklassen, 1992). Briefly, LEEM is a real time imaging technique, in which the surface of a sample under study is selectively probed using an electron beam incident at a very low energy, typically a few eV. The sample acts as one electrode of an immersion electron objective lens, which forms a real image of the illuminated region with the elastically reflected electrons. The low-energy electron diffraction pattern is easily accessible at the back focal plane of the objective lens, and is used to assign a structure to feature within the image.

The microscope used for these experiments was fabricated by the Arbeitsgruppe Bauer in Clausthal, Germany, and has been described elsewhere (Veneklassen, 1991). For these experiments, a nonspectroscopic form of the microscope was fitted with a magnetically focusing immersion objective lens, with a calculated resolution of approximately 100 Å (Chmelik et al., 1989). Heating during imaging is possible via electron bombardment from behind the sample. A number of grazing incidence ports give a clear view of the sample while positioned over the lens, making in situ evaporative deposition possible. The base pressure within the sample chamber of the microscope during the experiments was $2 \times 10^{-10}$ Torr.

Our silicon wafers were cut and polished to within 0.1° of the (1 1 1) orientation. Before introduction into the microscope, the samples were rinsed in reagent grade methanol, but not chemically etched. Further cleaning was via electron bombardment heating in UHV. Temperature was monitored with an infrared pyrometer, calibrated at the clean-surface Si (1 1 1)(7 × 7)– (1 × 1) transition (Bennett and Webb, 1981). Each sample was outgassed for several hours at a temperature of approximately 600°C, followed by rapid heating to approximately 1250°C, and fast cooling to approximately 900°C. The highest temperature was maintained for approximately 30 s, removing the oxide and sublimating away several hundred monolayers of silicon. LEEM images of the resulting surface showed an increased uniformity, if the extended heat treatment was followed by a very brief ''flash'' (approximately 1 s) to 1250°C.

Cobalt was deposited using evaporation from a resistively heated high purity wire. The amount deposited was measured in situ using a quartz crystal microbalance, calibrated at the saturation coverage of the ordered ($\sqrt{7} \times \sqrt{7}$) Co/Si (1 1 1) phase (Bennett et al., 1992a,b), of approximately 0.14 ML (1 ML = $7.8 \times 10^{14}$ atom/cm$^2$).

## 3. Results and discussion

Fig. 1 shows a series of images of a Si (1 1 1) surface during the deposition of cobalt at a temperature of 735°C, and an incident flux of 0.0018 ML/s. The first image is for the clean surface, which showed a sharp (7 × 7) LEED pattern. The image is featureless, and we identify the nearly uniform surface, imaged as light gray at these conditions, as (7 × 7) reconstructed. Almost immediately, on beginning to deposit Co onto the surface, regions of contrasting structure, nearly black at these conditions, appear in the image (panel (b)). This new structure segregates both to atomic height steps (which appear as long curved lines), and to domain boundaries between the different placements of the (7 × 7) reconstruction (which appear as shorter, nearly straight segments intersecting the steps). A disordered RC structure, also segregated to domain boundaries, was observed in STM images of Co/Si (1 1 1) which had been quenched to room temperature by Bennett et al., and which they refer to as the ''(1 × 1)''-RC structure (Bennett et al., 1992a). We identify

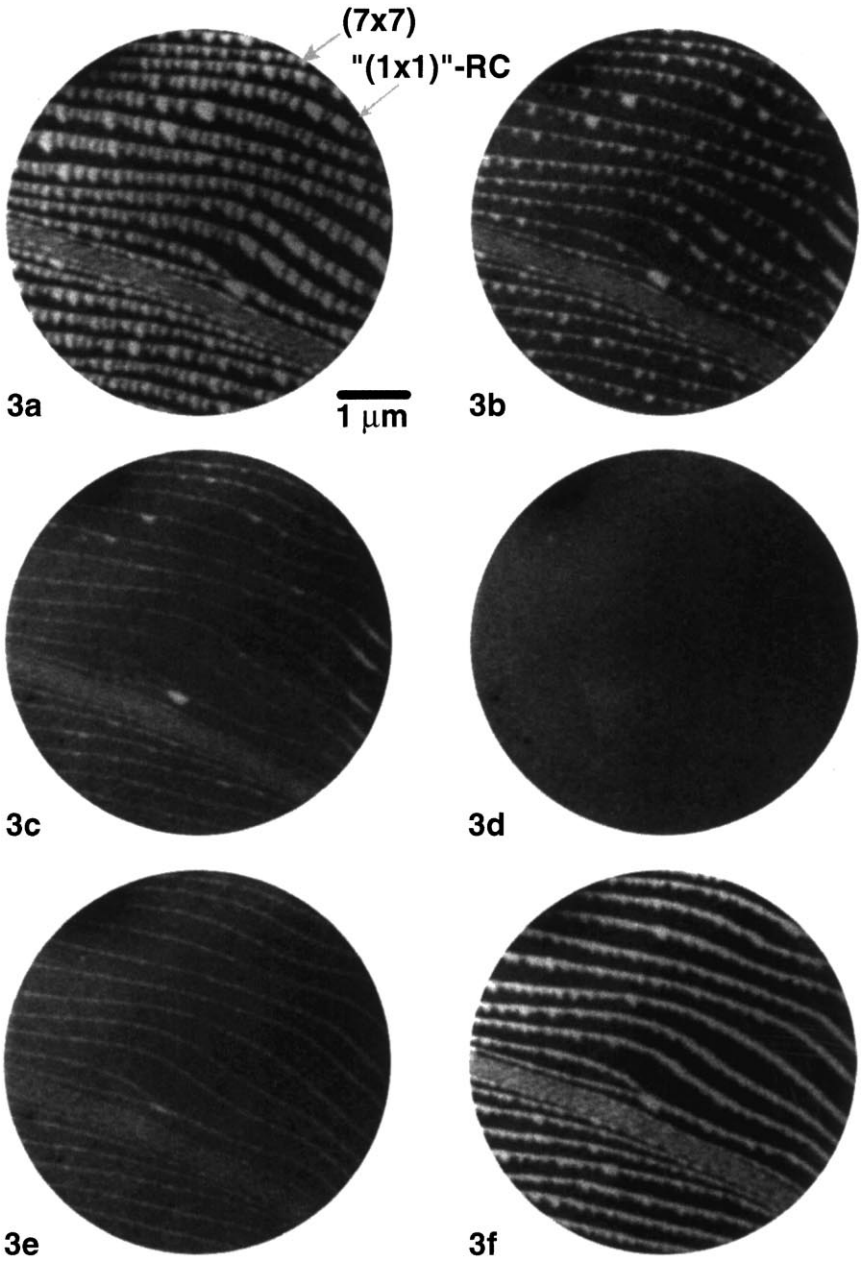


Fig. 3. LEEM images of Co/Si (1 1 1) for $\Theta_{Co} = 0.04$ ML during heating and cooling experiments, after incremental deposition of 0.004 ML. Scale bar shows 1 μm, $E_i = 3.6$ eV. Normal incidence. (a) $T = 768$°C (heating), (b) $T = 806$°C (heating), (c) $T = 816$°C (heating), (d) $T = 827$°C (heating), (e) $T = 816$°C (cooling), (f) $T = 768$°C (cooling).

the black regions in Fig. 1 as ''(1 × 1)''-RC structure, and confirmed this identification by the observation of a ''(1 × 1)'' LEED pattern (i.e. one showing only bulk-periodicity reflections) on surfaces covered by this structure. We have made qualitatively similar observations for the deposition of Ni on Si (1 1 1) previously (Bennett et al., 1995). The black regions in these images grow at the expense of the light (7 × 7)-reconstructed regions, covering all but the interiors of the largest (7 × 7) domains by a Co coverage of 0.1 ML (panel (d)). Beyond this coverage, yet a third contrasting structure, dark gray at these conditions, becomes visible in the images (panels (e) and (f)). It nearly covers the surface by a coverage of 0.14 ML, the approximate saturation coverage of the close-packed ($\sqrt{7} \times \sqrt{7}$)-RC structure. Small patches of ($\sqrt{7} \times \sqrt{7}$)-RC structure have earlier been seen in room temperature STM images (Bennett et al., 1992a). Fig. 2 shows the LEED pattern from the same region of the surface at a coverage of 0.22 ML. This LEED pattern contains all the reflections expected for the two possible azimuthal orientations of an ordered ($\sqrt{7} \times \sqrt{7}$) overlayer structure, identifying the dark gray regions as ($\sqrt{7} \times \sqrt{7}$)-RC. As previously noted (Phaneuf et al., 1997), the sequence of coexisting ordered and disordered structures shown in Figs. 1(a)–(f) is consistent with two-dimensional eutectic

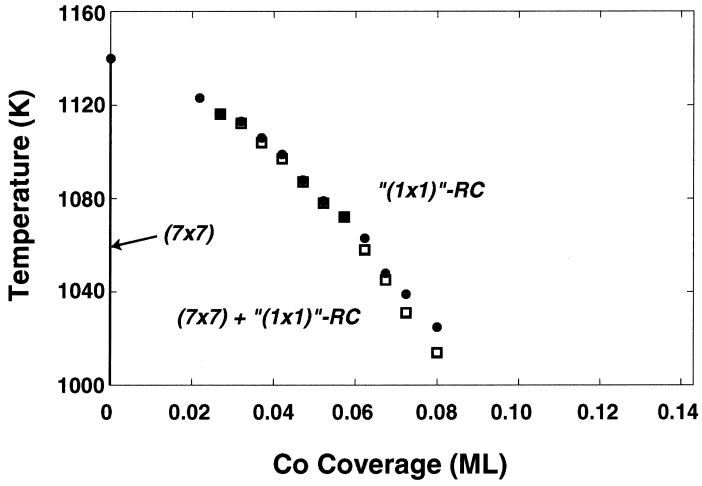


Fig. 4. Measured temperature at which (7 × 7) regions (white in Fig. 3) disappear on heating (solid circles) and reappear on cooling (open squares) versus Co coverage.

behavior, and indicates an insolubility of Co-containing RCs in the ordered (7 × 7) phase.

Beyond a coverage of approximately 0.14 ML small, nearly circular black regions become visible within the dark gray ($\sqrt{7} \times \sqrt{7}$) phase (panel (g)). As the Co coverage increases, small white ''islands'' become visible within some of these black regions (panel (h)). Turning off the incident Co flux, but maintaining the temperature, results in a rapid increase in the size of the black regions surrounding the islands. As discussed in the following, the small black regions are evidently the same ''(1 × 1)''-RC which forms immediately upon beginning to deposit Co onto the clean (7 × 7) surface. The reentrant appearance of this structure is apparently caused by the local depletion of surface Co by the nucleation and growth of islands a fourth phase, most likely $CoSi_2$ (Phaneuf, 1998).

To test for the reversibility of transitions between the ordered and disordered structures, we performed a series of experiments in which a small fraction of a monolayer of Co was deposited on the Si (1 1 1) surface, and then the temperature raised and lowered while imaging. Fig. 3 shows a series of LEEM images from a Si (1 1 1) surface on which a total of 0.04 ML of Co was deposited. In these images, the light gray regions are again (7 × 7) reconstructed, and the black regions are ''(1 × 1)''-RC. Panel (a) shows the surface after the last increment of 0.004 ML of Co deposition at 768°C. The (7 × 7) domains are nearly triangular, and are segregated to step edges. The shape is the same as that observed for the clean surface, on lowering the temperature through the (7 × 7)– ''(1 × 1)'' transition, and the direction of the apices of the triangles allows the orientation of the steps to be identified, as descending along a direction near the [$\underline{1}\,\underline{1}$ 2] (Telieps and Bauer, 1985). On heating the 0.04 ML-Co/Si (1 1 1) surface, the (7 × 7) domains shrink toward the step edges, and completely disappear at a temperature of approximately 824°C. The use of direct imaging, and the strong contrast between phases makes the assignment of this temperature unambiguous. Above this temperature, the surface is uniform ''(1 × 1)''-RC. On cooling, though the same temperature, (7 × 7) reconstructed regions reappear, nucleating at the step edges, and again showing a triangular domain growth shape. This reversibility with the temperature indicates a local equilibrium between the (7 × 7) and ''(1 × 1)''-RC phases (Phaneuf et al., 1997). The different appearance of the arrangement of the (7 × 7) domains in panels (a) and (f) indicates a limited range over which this equilibration occurs at the deposition temperature. The difference in appearance can be understood from the fact that the surface shown in panel (a) results from the deposition of Co onto a surface containing (7 × 7)-reconstructed regions which coalesced at the domain boundaries. The RCs segregate to the domain boundaries and grow outward. In contrast, the surface shown in panel (f) results from the nucleation of the (7 × 7) reconstruction at the step edges into a disordered phase, which has no such domain boundaries. Subsequent heating and cooling experiments after the first, at a fixed coverage, however produce essentially identical (7 × 7) domain shapes at a given temperature.

The measured (7 × 7)-disappearance temperatures on heating, and reappearance temperatures on cooling, over a range of Co coverages, are summarized in Fig. 4. The disappearance temperature is depressed by nearly 120°C from its clean-surface value by a coverage of only 0.08 ML. Above 780°C, the heating and cooling curves overlay upon one another. Beneath this temperature there is a slight hysteresis, perhaps indicating sluggish kinetics. The measured reversibility on multiple heating and cooling experiments at a fixed exposure indicates that it is possible to maintain a constant surface coverage over the time required for the measurements. This is most likely because of the exceedingly small bulk solubility of Co in Si (Weber, 1983) driving the surface out of equilibrium with the bulk for exceedingly small coverages. Such is not the case for Ni on Si (1 1 1)

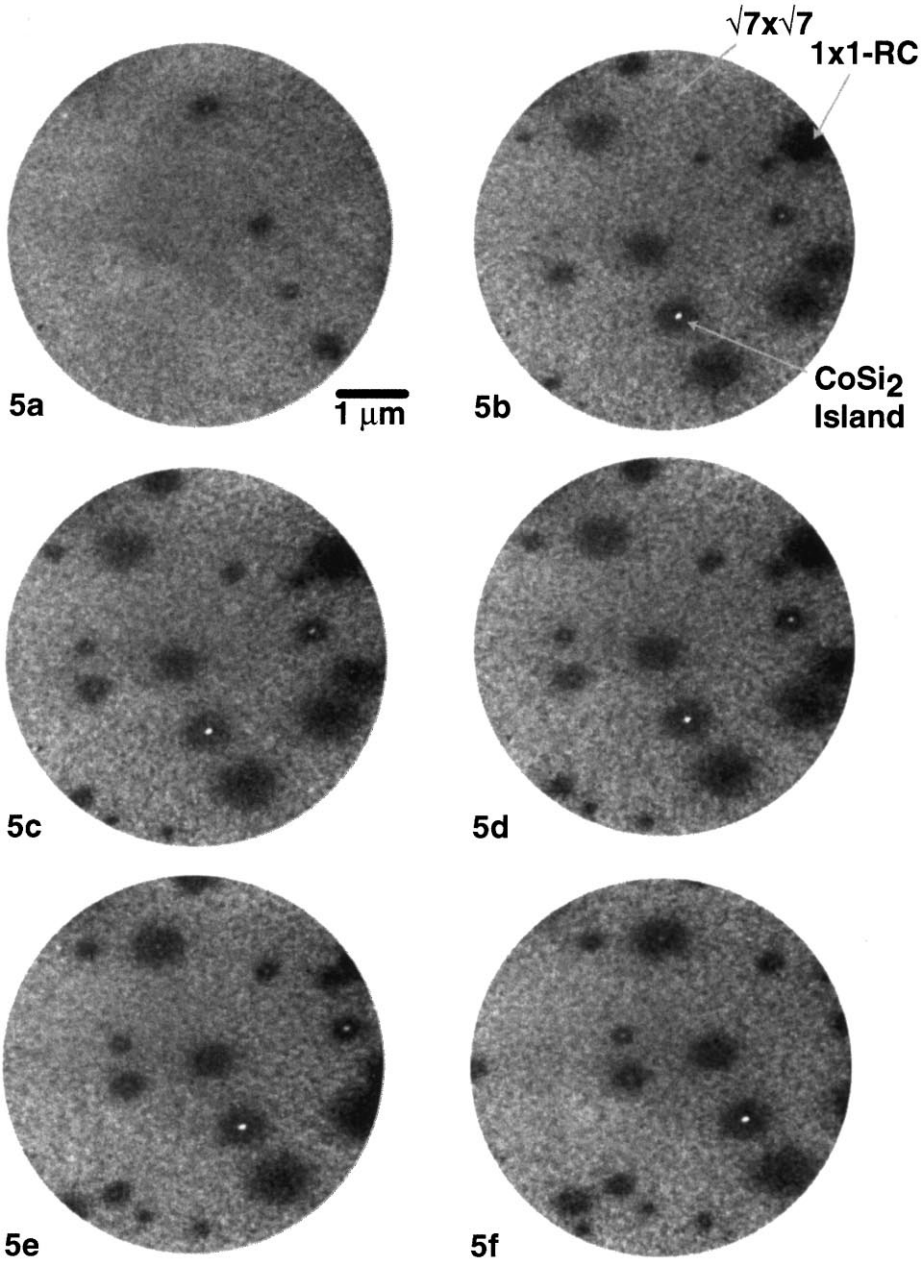


Fig. 5. LEEM images showing the irreversible transition of the ordered ($\sqrt{7} \times \sqrt{7}$)-RC to the disordered ''$(1 \times 1)$''-RC phase on heating and cooling. Scale bar shows 1 μm. $\Theta_{Co} = 0.13$ ML for all images. Incident flux turned off. Incident energy and angle and field of view as in Fig. 3. (a) $T = 670$°C (heating), (b) $T = 725$°C (heating), (c) $T = 740$°C (heating), (d) $T = 745$°C (heating), (e) $T = 725$°C (cooling), (f) $T = 670$°C (cooling).

(Bennett et al., 1995), in which the bulk solubility is much higher. A model based on the local equilibrium between surface phases is also consistent with the shape of the phase boundary which separates coexisting phases from uniform ''$(1 \times 1)$''-RC, and which is well fit by a simple equilibrium model for an interacting lattice gas of RCs (Phaneuf et al., 1997).

We also looked at the effect of changing the temperature at higher coverages corresponding to a coexistence between the ''$(1 \times 1)$''-RC and the ordered ($\sqrt{7} \times \sqrt{7}$) phase. Here however, we observed only irreversible transitions. Fig. 5 shows a series of images of a Si (1 1 1) surface on which 0.13 ML of Co was deposited, slightly less than the $\sqrt{7}$-saturation coverage, at a temperature of 670°C and a flux of 0.0003 ML. The ($\sqrt{7} \times \sqrt{7}$) structure, again dark gray in these images, covers the surface aside from a few roughly circular black regions of ''$(1 \times 1)$''-RC. These regions are several tenths of a micron across, considerably larger than the roughly 0.1 micron regions seen in Fig. 1(g), for which the deposition was at a higher flux and a lower temperature. Raising the temperature of this surface (panels (b)– (d)) results in the growth of these regions, and the formation

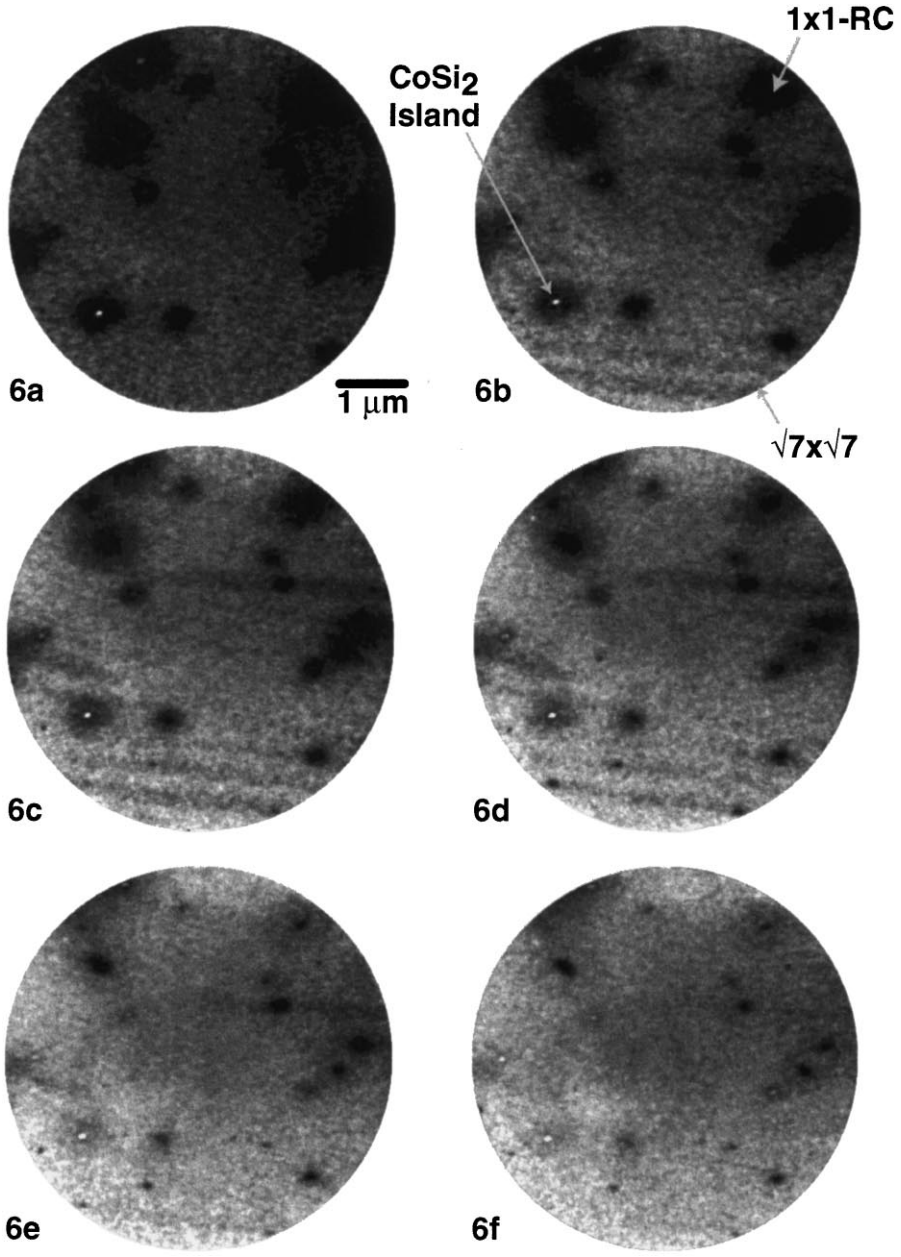


Fig. 6. LEEM images showing the disappearance of the ''(1 × 1)''-RC phase and regrowth of the ($\sqrt{7} \times \sqrt{7}$)-RC phase during the deposition of Co at a constant temperature. Scale bar shows 1 μm. $T = 670$°C. Incident flux is 0.0003 ML/s. (a) Elapsed deposition time, $t_e = 0$ s, $\Theta_{Co} = 0.130$ ML, (b) $t_e = 37$ s, $\Theta_{Co} = 0.141$ ML, (c) $t_e = 57$ s, 0.147 ML, (d) $t_e = 77$ s, $\Theta_{Co} = 0.153$ ML, (e) $t_e = 97$ s, $\Theta_{Co} = 0.159$ ML, (f) $t_e = 117$ s, $\Theta_{Co} = 0.165$ ML.

of new ones. In addition, very small contrasting (white) islands are observed to form within some of the ''(1 × 1)''-RC regions. Lowering the temperature of this surface (panels (e), (f)) does not reverse these changes, i.e. the islands do not disappear, and the circular ''(1 × 1)''-RC regions do not shrink.

A natural interpretation of this lack of reversibility is that very small islands of a stable phase, most likely $CoSi_2$, nucleate and grow at this coverage and temperature, depleting the surrounding region of the surface of Co. The observed replacement of the ($\sqrt{7} \times \sqrt{7}$) phase by the ''(1 × 1)''-RC is caused by the lower Co concentration within the latter phase. To test whether this interpretation is correct, we deposited additional Co onto this surface. The results are shown in Fig. 6. The ''(1 × 1)''-RC regions do indeed shrink and disappear, but the islands do not; in fact they appear to grow slightly. We find that the islands only disappear (irreversibly) after protracted heating at temperatures exceeding 1000°C. Our observations, shown in Figs. 5 and 6, are consistent with the circular, black regions as locally depleted of Co, and the islands as a stable high-coverage silicide phase. Recently, we confirmed this model directly using ESCA microscopy to measure the Co concentration in the vicinity of these islands, and to probe the stoichiometry

of the islands (Phaneuf, 1998). It is also interesting to note that the intensity in the dark gray regions in Fig. 6, increases during deposition. This indicates that the apparently uniform phase at the beginning of the additional deposition is, in fact, a finely dispersed mixture of coexisting ($\sqrt{7} \times \sqrt{7}$) and ''$(1 \times 1)$''-RC phases so that a larger fraction of these regions becomes ($\sqrt{7} \times \sqrt{7}$) during this sequence. The observation of intensity striations in these regions (panels (b) and (c)) which correlate with the underlying steps indicate either a tendency toward phase separation (as expected for a two-dimensional eutectic), or the selective nucleation of (unresolved) $CoSi_2$ islands along step edges, resulting in a local depletion of the surface Co concentration.

## 4. Conclusions

Si (1 1 1) undergoes a series of structural transitions during the deposition of Co at elevated temperatures. At surface Co coverages below 0.1 ML, a reversible phase separation indicates a local equilibrium between the ordered $(7 \times 7)$ and disordered ''$(1 \times 1)$''-RC phases. At coverages near1/7 ML only irreversible transitions are observable, because of the nucleation of islands of the stable $CoSi_2$ phase. These islands deplete the surface Co concentration locally, resulting in the disappearance of the Co-rich ordered ($\sqrt{7} \times \sqrt{7}$)-RC phase, and the formation of the lower Co concentration ''$(1 \times 1)$''-RC phase. The formation of islands of the stable silicide phase reduces the surface Co coverage and thus competes with a local equilibrium between surface phases.

The direct observation and characterization of both the reversible and irreversible transitions between the ordered and disordered structures during the deposition of Co on Si (1 1 1) was possible as a result of the ability to image this surface in real time, at high-temperature, and during growth using LEEM.

## Acknowledgements

It is a pleasure to acknowledge helpful conversations with Dr. N.C. Bartelt and Dr. M.Y. Lee. This work was supported by the NSF under Grant No. DMR9528503. One of us (RJP) received support from the Laboratory for Physical Sciences, and an NSF-MRSEC.

## References

Bartelt, N.C., Tromp, R.M., 1996. Low-energy electron microscopy study of step mobilities on Si (0 0 1). Phys. Rev. B 54, 11 731.

Bartelt, N.C., Theis, W., Tromp, R.M., 1996. Ostwald ripening of two-dimensional islands on Si (0 0 1). Phys. Rev. B 54, 11 741.

Bauer, E., Mundschau, M., Swiech, W., 1991. Low-energy electron microscopy of semiconductor surfaces. J. Vac. Sci. Technol. A 9, 1007.

Bauer, E., 1994. Low-energy electron microscopy. Rep. Prog. Phys. 57, 895.

Bennett, P.A., Webb, M.B., 1981. The Si (1 1 1) $7 \times 7$ to ''$(1 \times 1)$'' transition. Surface Sci. 104, 74.

Bennett, P.A., Copel, M., Cahill, D., Falta, J., Tromp, R.M., 1992. Ring clusters in transition-metal–silicon surface structures. Phys. Rev. Lett. 69, 1224.

Bennett, P.A., Devries, B., Robinson, I.K., Eng, P.J., 1992. Layerwise reaction at a buried interface. Phys. Rev. Lett. 69, 2539.

Bennett, P.A., Cahill, D.G., Copel, M., 1994. Initial precursor to silicide formation on Si (1 1 1)– $(7 \times 7)$. Phys. Rev. Lett. 73, 452.

Bennett, P.A., Lee, M.Y., Parikh, S.A., Würm, K., Phaneuf, R.J., 1995. Surface phase transformations in the Ni/Si (1 1 1) system real time observations using LEEM and STM. J. Vac. Sci. Technol. A 13, 1728.

Chmelik, J., Veneklassen, L.H., Marx, G., 1989. Comparing cathode lens configurations for low-energy electron microscopy. Optik 83, 155.

Mundschau, M., Bauer, E., Telieps, W., 1989. Atomic steps on Si (1 0 0) and step dynamics during sublimation studied by low-energy electron microscopy. Surface Sci. 223, 413.

Nicolet, M.A., Lau, S.S., 1983. Formation and characterization of transition-metal silicides. In: Einspruch, N. (Ed.). VLSI Electronics: Microstructure Science 6. Academic Press, New York, p. 330.

Phaneuf, R.J., Bartelt, N.C., Williams, E.D., Swiech, W., Bauer, E., 1991. Low-energy electron microscopy investigations of orientational phase separation on vicinal Si (1 1 1) surfaces. Phys. Rev. Lett. 67, 2986.

Phaneuf, R.J., Bartelt, N.C., Williams, E.D., Swiech, W., Bauer, E., 1992. Low-energy electron microscopy investigations of the domain growth of the $(7 \times 7)$ reconstruction on Si (1 1 1). Surface Sci. 268, 227.

Phaneuf, R.J., Bartelt, N.C., Williams, E.D., Swiech, W., Bauer, E., 1993. The crossover from metastable to unstable facet growth on Si (1 1 1). Phys. Rev. Lett. 71, 2284.

Phaneuf, R.J., Hong, Y., Horch, S., Bennett, P.A., 1997. Two-dimensional phase separation for Co adsorbed on Si (1 1 1). Phys. Rev. Lett. 78, 4605.

Phaneuf, R.J. et al., 1998, in preparation.

Reader, A.H., vanOmmen, A.H., Reis, P.J.W., Wolters, R.A.M., Oostra, D.J., 1993. Transition metal silicides in silicon technology. Rep. Prog. Phys. 56, 1397.

Swiech, W., Bauer, E., 1991. The growth of Si on Si (1 0 0): a video-LEEM study. Surface Sci. 255, 219.

Telieps, W., Bauer, E., 1985. The $(7 \times 7)$ to $(1 \times 1)$ transition on Si (1 1 1). Surface Sci. 162, 163.

Theis, W., Tromp, R.M., 1996. Nucleation in Si (0 0 1) homoepitaxial growth. Phys. Rev. Lett. 76, 2770.

Tu, K.N., Mayer, J.W., 1978. Silicide formation Thin Films-Interdiffusion and Reactions. Wiley, New York, p. 359.

Tung, R.T., 1992. Epitaxial $CoSi_2$ and $NiSi_2$ thin films. Materials Chem. Phys. 32, 107.

Tung, R.T., Batstone, J.L., 1988. Control of pinholes in epitaxial $CoSi_2$ layers on Si (1 1 1). Appl. Phys. Lett. 52, 648.

Veneklassen, L.H., 1991. Design of a spectroscopic low-energy electron microscope. Ultramicr. 36, 76.

Veneklassen, L.H., 1992. The continuing development of low-energy electron microscopy for imaging surfaces. Rev. Sci. Instrum. 63, 5513.

Weber, E., 1983. Transition metals in silicon. Appl. Phys. A 30, 1.